STIMULUS REPORT

blood advances

Intratumoral T cells have a differential impact on FDG-PET parameters in follicular lymphoma

Karthik Nath,[1] Soi-Cheng Law,[1] Muhammed B. Sabdia,[1] Jay Gunawardana,[1] Lilia M. de Long,[1] David Sester,[2] Mohamed Shanavas,[1] Hennes Tsang,[1] Joshua W. D. Tobin,[1] Sarah-Jane Halliday,[3] Annette Hernandez,[3] Donna Cross,[3] Robert J. Bird,[3] Sanjiv Jain,[4] Colm Keane,[1,3] Dipti Talaulikar,[5,6] Judith Trotman,[7,8] Phillip Law,[9] and Maher K. Gandhi[1,3]

[1]Mater Research Institute, University of Queensland, Brisbane, QLD, Australia; [2]TRI Flow Cytometry Suite, Translational Research Institute, Brisbane, QLD, Australia; [3]Department of Haematology, Princess Alexandra Hospital, Brisbane, QLD, Australia; [4]ACT Pathology, Canberra Hospital, Canberra, ACT, Australia; [5]Haematology Translational Research Unit, Canberra Hospital, Canberra, ACT, Australia; [6]Australian National University, Canberra, ACT, Australia; [7]Department of Haematology, Concord Repatriation General Hospital, Concord, NSW, Australia; [8]University of Sydney, Concord, NSW, Australia; and [9]Department of Medical Imaging, Princess Alexandra Hospital, Brisbane, QLD, Australia

Key Points

- Pretherapy TMTV is reflective of the FL tumor cell burden within malignant nodes.
- Glucose-avid intratumoral T cells influence pretherapy SUV_{max} in FL.

Data on the prognostic impact of pretherapy ^{18}F-fluorodeoxyglucose–positron emission tomography (FDG-PET) in follicular lymphoma (FL) is conflicting. The predictive utility of pretherapy total metabolic tumor volume (TMTV) and maximum standardized uptake value (SUV_{max}) on outcome appears to vary between regimens. Chemoimmunotherapies vary in the extent of T-cell depletion they induce. The role of intratumoral T cells on pretherapy FDG-PET parameters is undefined. We assessed pretherapy FDG-PET parameters and quantified intratumoral T cells by multiple methodologies. Low intratumoral T cells associated with approximately sixfold higher TMTV, and FL nodes from patients with high TMTV showed increased malignant B-cell infiltration and fewer clonally expanded intratumoral $CD8^+$ and $CD4^+$ T-follicular helper cells than those with low TMTV. However, fluorescently labeled glucose uptake was higher in $CD4^+$ and $CD8^+$ T cells than intratumoral B cells. In patients with FDG-PET performed prior to excisional biopsy, SUV_{max} within the subsequently excised node associated with T cells but not B cells. In summary, TMTV best reflects the malignant B-cell burden in FL, whereas intratumoral T cells influence SUV_{max}. This may contribute to the contradictory results between the prognostic role of different FDG-PET parameters, particularly between short- and long-term T-cell–depleting chemoimmunotherapeutic regimens. The impact of glucose uptake in intratumoral T cells should be considered when interpreting pretherapy FDG-PET in FL.

Introduction

The identification of patients with follicular lymphoma (FL) that is destined to respond poorly to frontline therapy remains elusive.[1] To this end, quantifiable pretherapy ^{18}F-fluorodeoxyglucose-positron emission tomography-computed tomography (FDG-PET) imaging parameters have been evaluated to identify such high-risk patients. The parameters include total metabolic tumor volume (TMTV), which gives insight into the burden of the tumor by 3-dimensional quantification encompassing all involved sites, and maximum standardized uptake value (SUV_{max}), a standardized measure of the highest FDG-uptake within a single

Submitted 16 December 2020; accepted 3 April 2020; published online 22 June 2021.
DOI 10.1182/bloodadvances.2020004051.

Presented in abstract form at the 16th International Conference on Malignant Lymphoma, 22 June 2021.

DNA/RNA sequencing was not performed. The NanoString features are in supplemental Tables 3 and 4. For original data, please contact Karthik Nath (karthik.nath@uqconnect.edu.au).

The full-text version of this article contains a data supplement.

lesion. Pooled analyses of predominantly cyclophosphamide, doxorubicin, vincristine, and prednisone+ rituximab (R-CHOP)–treated patients (of whom only a subset received R maintenance) found that increased pretherapy TMTV is a strong predictor of an adverse outcome in FL.[2,3] Interestingly, in the same group of treated patients, both a low and high SUV_{max} have been associated with a reduced progression-free survival (PFS).[4,5] However, FDG-PET analysis of the phase 3 GALLIUM study (58% treated by bendamustine induction), in which all patients received anti-CD20 antibody maintenance, found no association with either TMTV or SUV_{max}.[6] Intriguingly, high pretherapy SUV_{max} was associated with shorter PFS in nonanthracycline-treated (mainly bendamustine or lenalidomide) but not in anthracycline (R-CHOP)–treated patients in another study.[7]

The predictive utility of a pretherapy T-effector gene signature in patients treated with CHOP/CVP (cyclophosphamide, vincristine, prednisone)-rituximab/obinutuzumab is reversed in patients treated with bendamustine-rituximab (B-R)/obinutuzumab.[8] Unlike R-CHOP, B-R causes profound and sustained T-cell depletion.[9] Rituximab maintenance after B-R induction may prolong $CD4^+$ T-cell lymphopenia,[10] involving reduced production of interleukin-17 and -15, which are critical for survival of $CD4^+$ T-cell memory.[11] The extent to which clonally expanded T cells infiltrate the tumor microenvironment (TME) in FL is also prognostic.[12] Notably, the TME is distinct from that of other non-Hodgkin and Hodgkin lymphomas, with a high population of $CD4^+$ T-follicular helper cells (T_{FH}).[13] Although the FDG-tracer detects cellular glucose-uptake by all viable cells within the tumor site, to our knowledge, the role of intratumoral T cells on pretherapy FDG-PET parameters in FL remains undefined. Potentially, differences in the prognostic impact between SUV_{max} and TMTV in FL across studies, may in part reflect the differential depletion of glucose-avid intratumoral T cells after exposure to different chemoimmunotherapeutic regimens.

FDG-PET is integral to FL management. In this study, we assessed the relationship of TMTV and SUV_{max} with intratumoral T cells in FL. The findings have implications for the improved interpretation of FDG-PET metrics in FL, which remains an unmet need in this disease.

Methods

The study was approved by the institutional regulatory board (Metro South Human Research Ethics Committee) and was conducted in concordance with the Declaration of Helsinki. Eighty-three patients with histologically confirmed de novo grade 1 to 3a FL were included (characteristics in Table 1). The consort diagram (supplemental Figure 1) outlines sample testing, which was based solely on availability.

Pretherapy FDG-PET scans were assessed for SUV_{max}, TMTV, and total lesion glycolysis (TLG), using customized software (MIM Software, Cleveland, OH).[6,14,15] Biopsy samples (formalin-fixed, paraffin-embedded tissue and tumor-infiltrating lymphocytes [TILs] from deaggregated nodes) were used for multiplex gene hybridization, immunohistochemistry, T-cell receptor (TCR) repertoire sequencing and flow cytometry as published.[12,16-19] Cryopreserved TILs were used to assess cellular glucose uptake by intratumoral $CD4^+$ T cells, $CD8^+$ T cells, and $CD19^+$ B cells, by using the fluorescently

Table 1. Patient baseline characteristics in the Brisbane and Canberra cohorts

	Brisbane (n = 63)	Canberra (n = 20)
Age, y		
Median	62	66
Range	29-84	43-87
>60	34 (55)	14 (67)
Sex		
Female	27 (43)	12 (60)
Male	36 (57)	8 (40)
Ann Arbor stage		
I-II	10 (16)	1 (6)
III-IV	53 (84)	18 (94)
LDH		
Normal	46 (73)	10 (53)
>ULN	17 (27)	9 (47)
Hemoglobin, g/dL		
≥12	47 (75)	16 (80)
<12	16 (25)	4 (20)
Nodal involvement, n		
≦4	24 (38)	3 (17)
>4	39 (62)	15 (83)
Grade		
1-2	55 (87)	13 (65)
3A	8 (13)	7 (35)
Ki67 by IHC, %		
<20	23 (70)	–
≥20	10 (30)	–
FLIPI		
0	2 (3)	
1	7 (11)	
2	25 (40)	6 (33)
3	19 (30)	8 (44)
4	6 (10)	4 (22)
5	4 (6)	–
Initial treatment		
R-chemo	42 (66)	10 (50)
Observation	15 (24)	5 (25)
O-chemo	2 (3)	3 (15)
R-mono	1 (2)	2 (10)
XRT only	3 (5)	0 (0)
Maintenance therapy		
Yes	33 (52)	9 (45)
No	30 (48)	11 (55)

Data are expressed as the number (percentage) of patients in the subgroups, unless otherwise stated.

FLIPI, Follicular Lymphoma International Prognostic Index; IHC, immunohistochemistry; LDH, lactate dehydrogenase; maintenance therapy, maintenance anti-CD20 monoclonal antibody therapy; O-chemo, obinutuzumab chemotherapy; R-chemo, rituximab chemotherapy; R-mono, rituximab monotherapy; ULN, upper limit of normal; XRT, radiation therapy.

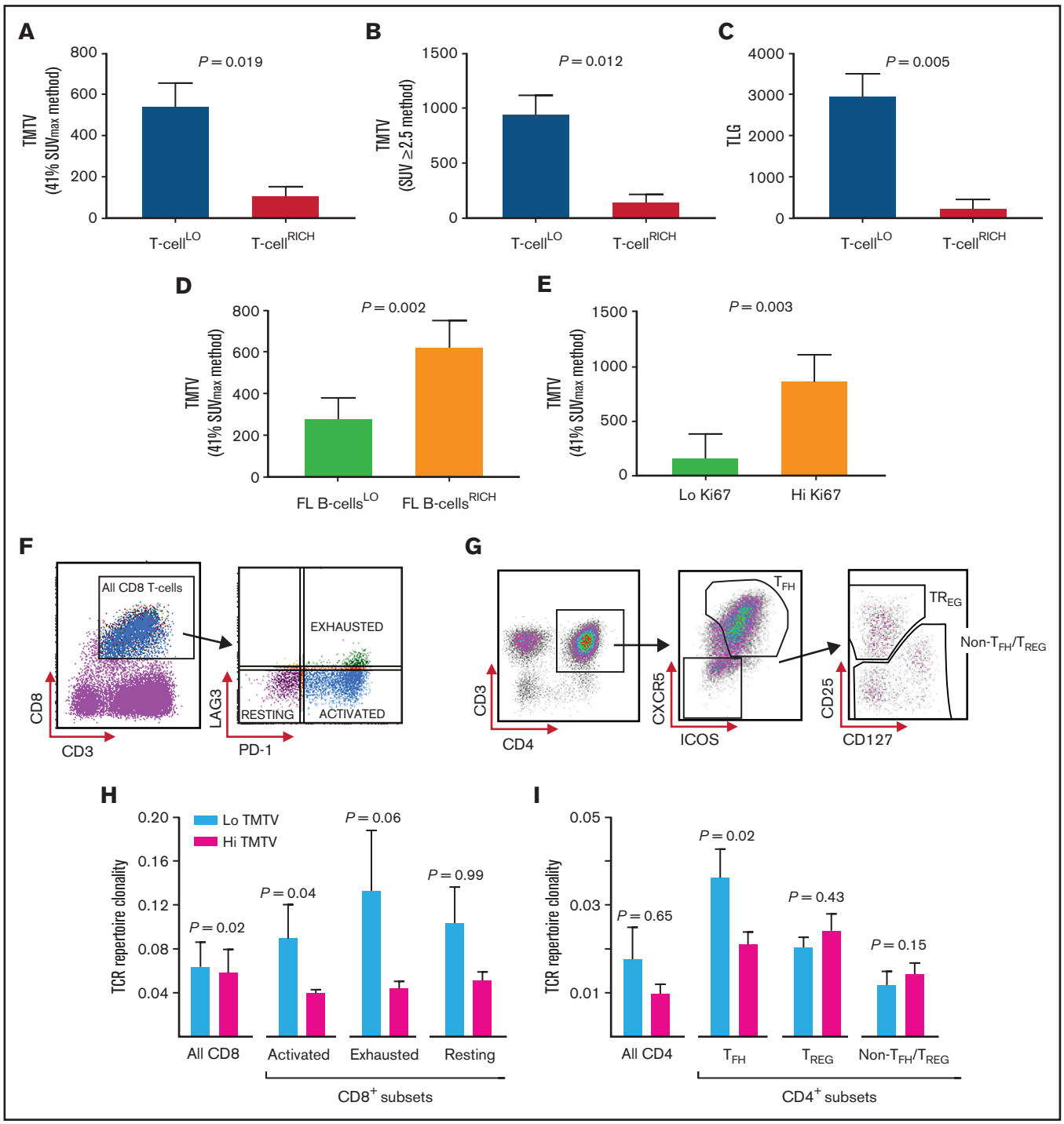

Figure 1. Analyses of the biologic determinants of TMTV in FL. (A) TMTV (in cubic centimeters), determined by 41% SUV_{max}, in patients with T-cell^{LO} or T-cell^{RICH} infiltrate in the nodes. T-cell infiltrative states were measured by calculating a standardized *CD4* and *CD8A* gene *z*-score for each sample by multiplex gene hybridization. T-cell^{LO}: quartiles 1-3; n = 34. T-cell^{RICH}: quartile 4; n = 11. (B) TMTV, determined by SUV ≥2.5, in patients with T-cell^{LO} and T-cell^{RICH} tumors. (C) TLG (in grams), in patients with a T-cell^{LO} or T-cell^{RICH} tumor infiltrate. (D) TMTV in patients with a low (FL B cells^{LO}; n = 27) or high (FL B cells^{RICH}, n = 27) intratumoral FL B-cell infiltrate. FL B-cell infiltration was quantified by a median cutoff for the percentage of light-chain–restricted CD19$^+$ FL B cells (≦60%), by using flow cytometric quantification of tumor lymphocytes in 54 fresh tissue samples. TMTV was determined by the 41% SUV_{max} method. (E) TMTV in patients with a low Ki67 expression (<20%; n = 23), and high Ki67 expression (≥20%; n = 10). Ki67 expression was assessed by immunohistochemistry, and a 20% cutoff threshold was chosen, as previously published.[25] (F) Gating strategy for CD8$^+$ T-cell subsets obtained from cryopreserved FL TIL samples to allow for the identification of PD-1$^+$LAG3$^-$ (activated, ~58% CD8$^+$ cells), PD-1$^+$LAG3$^+$ (exhausted, ~18%), and PD-1$^-$LAG3$^-$ (resting, ~24%) intratumoral CD8$^+$ cell subsets by fluorescence-activated cell sorting (FACS). (G) Gating strategy for intratumoral CD4$^+$ T-cell subsets obtained from FL TIL samples to allow for the identification of CXCR5$^+$ICOS$^+$CD4$^+$ T_{FH} cells, and CD25^{HI}CD127^{LO}CXCR5$^-$CD4$^+$

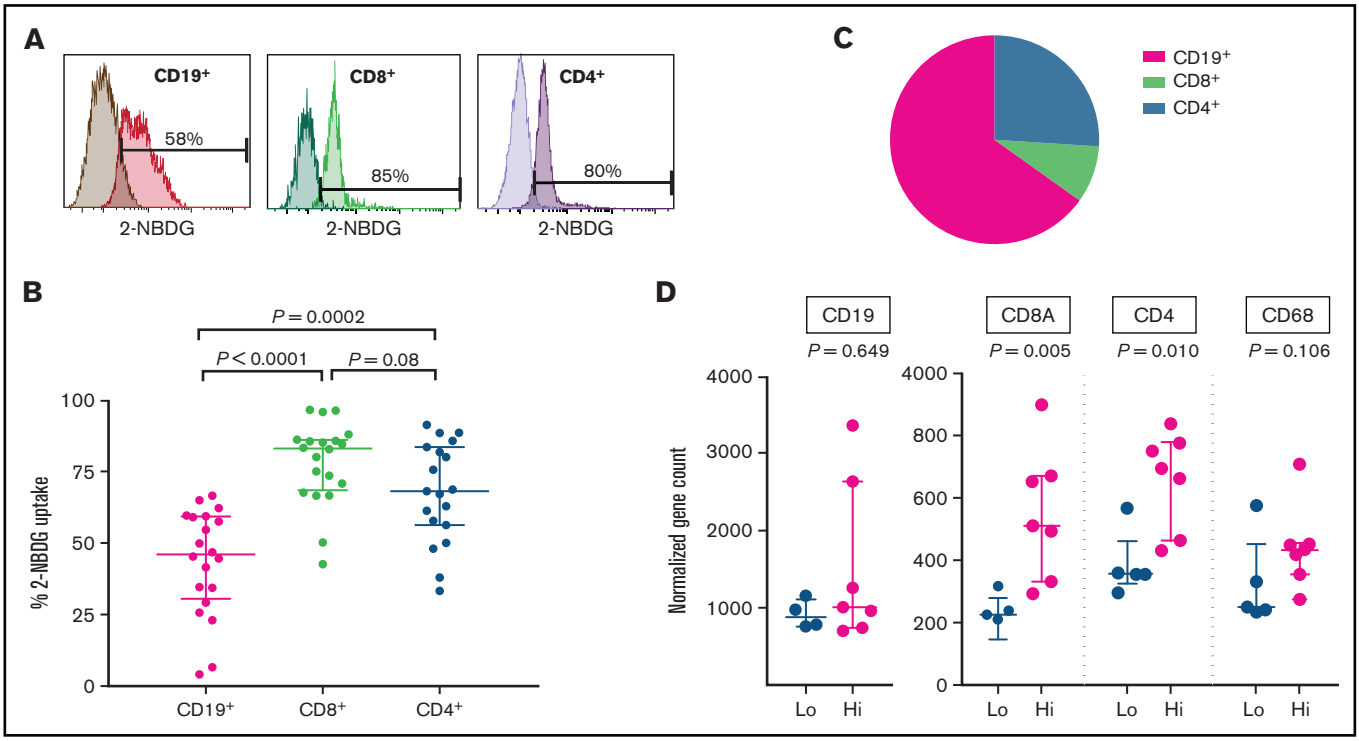

Figure 2. Assessment of cellular glucose uptake within intratumoral lymphocyte subsets and determinants of $SUV_{lesional}$. (A) Representative 2-NBDG uptake of intratumoral $CD19^+$, $CD8^+$, and $CD4^+$ cells, by flow cytometry. 2-NBDG, a fluorescently tagged FDG analogue, was used to determine cellular glucose uptake. Darker shades represent negative controls. There was a strong correlation between intratumoral $CD19^+$ cells and light-chain–restricted monoclonal $CD19^+$ FL tumor cells (Spearman $r = 0.97$; $P < .0001$), and hence intratumoral $CD19^+$ cells were representative of FL B cells. (B) Combined results from 20 FL TIL samples of 2-NBDG uptake within intratumoral $CD19^+$, $CD8^+$, and $CD4^+$ cells. (C) Percentage lymphocyte contribution to overall glucose uptake after normalizing for the fraction of $CD19^+$, $CD8^+$, and $CD4^+$ live cells within each of the FL TILs. Average live cell infiltration: $CD19^+$ cells, ~64%; $CD8^+$ cells, ~4%; and $CD4^+$ cells, ~18%. (D) Twelve patients with prebiopsy FDG-PET scans had SUV_{max} obtained from their subsequently excised lymph node ($SUV_{lesional}$). $SUV_{lesional}$ values were categorized into a low and high state using a mean cutoff threshold (mean $SUV_{lesional}$, 6.5). Lymphocyte (*CD19*, *CD8A*, and *CD4*) and macrophage (*CD68*) gene infiltration was assessed within subsequently excised lymph node tissue samples by multiplex gene hybridization. Gene counts are reported according to the prebiopsy $SUV_{lesional}$ state. The Wilcoxon rank-sum test was used for all analyses.

labeled glucose analogue 2-NBDG uptake assay (Abcam).[20] The supplemental Methods provides a detailed description.

Results and discussion

Multiplex gene hybridization was used to quantify intratumoral T-cell infiltration in 45 patients with FL and compared with TMTV. T-cell infiltration was calculated by a standardized *CD4* and *CD8A* gene *z*-score, with $T\text{-cell}^{LO}$ defined as quartiles 1 to 3 ($n = 34$), and $T\text{-cell}^{RICH}$ as quartile 4. Patients with a $T\text{-cell}^{LO}$ state had a significantly higher TMTV than $T\text{-cell}^{RICH}$ (approximately fivefold, using the 41% SUV_{max}, and approximately sixfold using SUV ≥2.5; Figure 1A-B). TLG was also significantly higher in $T\text{-cell}^{LO}$ states (approximately sevenfold; Figure 1C). Next, proportions of clonal (light-chain restricted) B cells and $CD4^+$ and $CD8^+$ T cells were enumerated by flow cytometry in 54 fresh nodal tissues. Those with greater than the median cutoff of FL B cells within tumor biopsy specimens ($FL\ B\ cells^{RICH}$) had approximately twofold higher TMTV than those with $FL\ B\ cells^{LO}$ (Figure 1D). High Ki67 was also associated with increased TMTV (Figure 1E). However, TMTV was not associated with histological grade (1 and 2 vs 3A) or serum lactate dehydrogenase (supplemental Figure 2). Put together, the results indicate that TMTV reflects the burden of malignant B cells within FL nodes, which explains its inverse association with T-cell infiltration.

T cells proliferate in response to antigenic stimulation into clonally expanded populations.[21] Therefore, glucose metabolism may differ because of the degree of clonal expansions within T-cell compartments, reflected in differential TMTV. There are currently no data on the relationship between T-cell clonality in specific T-cell subsets and TMTV in FL. In 21 FL TILs, sorted into $CD8^+$ T-cell (Figure 1F),

Figure 1. (continued) T_{REG} and $CD4^+$ non-T_{FH}/T_{REG} subsets within the $CXCR5^-ICOS^-$ population by FACS. (H) Intratumoral $CD8^+$ (n = 21) and $CD8^+$ cell-subset–specific (n = 14) TCR repertoire clonality, as determined by Simpson's clonality metric, in patients with a low TMTV (n = 10 for $CD8^+$, and n = 8 for $CD8^+$ subset-specific cells) and those with a high TMTV (n = 11 for $CD8^+$, and n = 6 for $CD8^+$ subset-specific cells). A median TMTV cutoff threshold (268 cm^3) was used to distinguish a low from a high TMTV (by the 41% SUV_{max} method). (I) TCR repertoire clonality in patients with a low TMTV (n = 10) and patients with a high TMTV (n = 11) within the sorted intratumoral $CD4^+$ cell subsets. The Wilcoxon rank-sum test was used for all analyses.

T_{FH} cell, regulatory T-cell (T_{REG}), and non-T_{FH}/T_{REG} $CD4^+$ T-cell (Figure 1G) subsets, TCR sequencing showed that large T-cell clones predominantly resided in the $CD8^+$ T-cell population (mean clonality index [Clx], 0.067; ~33% of all T cells). T-cell clonality was intermediate in T_{FH} cells (Clx, 0.029; ~30% of all T cells), low in T_{REG} (Clx, 0.022; ~7%), and lowest in non-T_{FH}/T_{REG} cells (Clx, 0.013; ~31%). Importantly, there was modest enrichment of expanded T_{FH} and $CD8^+$ T-cell clones in low TMTV states (Figure 1H-I). Further interrogation of the intratumoral $CD8^+$ T-cell population suggested that the clonal expansions were primarily driven by activated, rather than exhausted or resting, $CD8^+$ T-cell subsets (Figure 1H). These findings require validation in larger, independent cohorts.

To evaluate the relative contribution of intratumoral B and T cells to TMTV, 2-NBDG was used to determined cellular glucose uptake in TILs (Figure 2A). The $CD8^+$ and $CD4^+$ T cells had significantly higher glucose uptake than did the $CD19^+$ B cells (Figure 2B). However, given that $CD19^+$ B cells contribute approximately two-thirds of the total lymphocyte population, it was the B cells that contributed the most to overall glucose uptake (Figure 2C). This further supports our initial finding that TMTV is reflective of the burden of the malignant population. Notably, cellular metabolism of TILs may be altered by cryopreservation and subsequent thawing. Experiments in fresh TILs are needed to confirm our findings.

Finally, we assessed SUV_{max}. TMTV is a volumetric assessment, whereas SUV_{max} is a measure of highest FDG avidity. Therefore, the contribution of the TME to SUV_{max} may differ from that of TMTV. To accurately assess the difference, we identified a subset of patients with FDG-PET imaging before their diagnostic FL biopsy, from which we obtained $SUV_{lesional}$ (ie, SUV_{max} within the subsequently excised node) values. After excisional biopsy, we assessed immune gene infiltration by multiplex gene hybridization and cellular glucose uptake and compared the results with the paired $SUV_{lesional}$ value. Those with high $SUV_{lesional}$ values had significantly higher *CD4* and *CD8A*, but not *CD19* gene expression (Figure 2D). Unsurprisingly (as macrophages make up only a small percentage of the TME),[12] there was no association with *CD68*. There was a trend toward a positive correlation between $CD4^+$, but not $CD8^+$ or $CD19^+$, cellular glucose uptake and $SUV_{lesional}$ (supplemental Table 1). These results demonstrate that intratumoral T cells play an important role in SUV_{max} of individual FL lesions. Intratumoral T-cell spatial heterogeneity, with T_{FH} cells particularly pronounced, is an established feature of FL[22,23] and may influence SUV variability between lesions to contribute to the inconsistent prognostic efficacy of SUV_{max}. It may also influence the potential inability of pretherapy SUV_{max} to predict subsequent histological transformation.[24]

In conclusion, our study suggests that intratumoral T cells differentially influence pretherapy FDG-PET parameters and can affect the predictive utility of FDG-PET in patients with FL who are treated with different chemoimmunotherapy regimens that vary in the extent of T-cell depletion that they induce. How chemotherapy-free immunomodulatory and/or checkpoint blockade therapies influence glucose-uptake in intratumoral T cells to affect interim and end-of-therapy FDG-PET parameters in FL is another avenue to be explored.

Acknowledgments

The visual abstract was created with Biorender.com. No writing assistance was used in the production of the manuscript.

This work was supported by a Haematology Society of Australia and New Zealand and Leukaemia Foundation scholarship (K.N.); the Leukaemia Foundation, the Mater Foundation, and the National Health and Medical Research Council (M.K.G.); and the Translational Research Institute FACSymphony A5 Reagent Support Fund which supported panel development. The Translational Research Institute is supported by the Australian Government.

Authorship

Contribution: K.N., S.-C.L., and P.L. contributed to the study design, performed the experiments and collected and analyzed the data; M.B.S., J.G., L.M.d.L., D.S., M.S., H.T., J.W.D.T., S.-J.H., A.H., and D.C. performed experiments and contributed to data interpretation; S.J., R.J.B., and D.T. provided patient samples, collected data and contributed to data interpretation; C.K. and J.T. contributed to data analysis and interpretation; M.K.G. designed the project and contributed to patient samples and data analysis and interpretation; and all authors were involved in writing the manuscript.

Conflict-of-interest disclosure: D.T. has received research funding, honoraria and has held an advisory board membership from Amgen; honoraria and speakers bureau and advisory board membership for Janssen; honoraria for Novartis; honoraria, speakers' bureau, and advisory board membership for Roche; and honoraria for Takeda. M.K.G. has received honoraria and travel support from Roche and honoraria from Janssen, Merck, Amgen, and Gilead. The remaining authors declare no competing financial interests.

ORCID profiles: ORCID profiles: K.N: 0000-0002-3881-5681; S-C.L: 0000-0002-0782-6951; M.B.S: 0000-0003-1977-8878; J.G: 0000-0003-2695-3849; L.M.d.L: 0000-0002-6989-8424; M.S: 0000-0001-6558-1721; H.T: 0000-0002-4340-2531; J.W.D.T: 0000-0003-4982-525X; R.B: 0000-0002-3110-1424; C.K: 0000-0002-9009-9934; D.T: 0000-0001-6766-8345; J.T: 0000-0001-8009-4593; P.L: 0000-0002-3905-5565; MKG: 0000-0003-1000-5393

Correspondence: Karthik Nath, Level 7, Translational Research Institute, Brisbane, QLD 4102, Australia; e-mail: karthik.nath@uqconnect.edu.au; and Maher K. Gandhi, Level 7, Translational Research Institute, Brisbane, QLD 4102, Australia; e-mail: maher.gandhi@mater.uq.edu.au.

References

1. Casulo C, Nastoupil L, Fowler NH, Friedberg JW, Flowers CR. Unmet needs in the first-line treatment of follicular lymphoma. *Ann Oncol.* 2017;28(9):2094-2106.

2. Meignan M, Cottereau AS, Versari A, et al. Baseline Metabolic Tumor Volume Predicts Outcome in High-Tumor-Burden Follicular Lymphoma: A Pooled Analysis of Three Multicenter Studies. *J Clin Oncol.* 2016;34(30):3618-3626.

3. Delfau-Larue M-H, van der Gucht A, Dupuis J, et al. Total metabolic tumor volume, circulating tumor cells, cell-free DNA: distinct prognostic value in follicular lymphoma. *Blood Adv.* 2018;2(7):807-816.

4. Cottereau AS, Versari A, Chartier L, et al. Low suvmax measured on baseline FDG-PET/CT and elevated β2 microglobulin are negative predictors of outcome in high tumor burden follicular lymphoma treated by immunochemotherapy: a pooled analysis of three prospective studies [abstract]. *Blood.* 2016;128(22). Abstract 1101.

5. Rossi C, Tosolini M, Gravelle P, et al. Baseline SUVmax is related to tumor cell proliferation and patient outcome in follicular lymphoma [published online ahead of print 17 December 2020]. *Haematologica.* 2020.

6. Barrington SF, Trotman J, Sahin D, et al. Baseline PET-Derived Metabolic Tumor Volume Metrics Did Not Predict Outcomes in Follicular Lymphoma Patients Treated with First-Line Immunochemotherapy and antibody maintenance in the phase III GALLIUM study [abstract]. *Blood.* 2018;132(suppl 1). Abstract 2882.

7. Strati P, Ahmed MA, Fowler NH, et al. Pre-treatment maximum standardized uptake value predicts outcome after frontline therapy in patients with advanced stage follicular lymphoma. *Haematologica.* 2020;105(7):1907-1913.

8. Bolen CR, Mattiello F, Herold M, et al. Treatment dependence of prognostic gene expression signatures in de novo follicular lymphoma [letter]. *Blood.* 2021;blood.2020008119.

9. Flinn IW, van der Jagt R, Kahl BS, et al. Randomized trial of bendamustine-rituximab or R-CHOP/R-CVP in first-line treatment of indolent NHL or MCL: the BRIGHT study. *Blood.* 2014;123(19):2944-2952.

10. Yutaka T, Ito S, Ohigashi H, et al. Sustained CD4 and CD8 lymphopenia after rituximab maintenance therapy following bendamustine and rituximab combination therapy for lymphoma. *Leuk Lymphoma.* 2015;56(11):3216-3218.

11. Misumi I, Whitmire JK. B cell depletion curtails CD4+ T cell memory and reduces protection against disseminating virus infection. *J Immunol.* 2014;192(4):1597-1608.

12. Tobin JWD, Keane C, Gunawardana J, et al. Progression of Disease Within 24 Months in Follicular Lymphoma Is Associated With Reduced Intratumoral Immune Infiltration. *J Clin Oncol.* 2019;37(34):3300-3309.

13. Scott DW, Gascoyne RD. The tumour microenvironment in B cell lymphomas. *Nat Rev Cancer.* 2014;14(8):517-534.

14. Boellaard R, Delgado-Bolton R, Oyen WJG, et al; European Association of Nuclear Medicine (EANM). FDG PET/CT: EANM procedure guidelines for tumour imaging: version 2.0. *Eur J Nucl Med Mol Imaging.* 2015;42(2):328-354.

15. Ilyas H, Mikhaeel NG, Dunn JT, et al. Defining the optimal method for measuring baseline metabolic tumour volume in diffuse large B cell lymphoma. *Eur J Nucl Med Mol Imaging.* 2018;45(7):1142-1154.

16. Keane C, Gill D, Vari F, Cross D, Griffiths L, Gandhi M. CD4(+) tumor infiltrating lymphocytes are prognostic and independent of R-IPI in patients with DLBCL receiving R-CHOP chemo-immunotherapy. *Am J Hematol.* 2013;88(4):273-276.

17. Keane C, Gould C, Jones K, et al. The T-cell Receptor Repertoire Influences the Tumor Microenvironment and Is Associated with Survival in Aggressive B-cell Lymphoma. *Clin Cancer Res.* 2017;23(7):1820-1828.

18. Yang ZZ, Kim HJ, Villasboas JC, et al. Expression of LAG-3 defines exhaustion of intratumoral PD-1$^+$ T cells and correlates with poor outcome in follicular lymphoma. *Oncotarget.* 2017;8(37):61425-61439.

19. Yang Z-Z, Kim HJ, Wu H, et al. TIGIT Expression Is Associated with T-cell Suppression and Exhaustion and Predicts Clinical Outcome and Anti-PD-1 Response in Follicular Lymphoma. *Clin Cancer Res.* 2020;26(19):5217-5231.

20. Zou C, Wang Y, Shen Z. 2-NBDG as a fluorescent indicator for direct glucose uptake measurement. *J Biochem Biophys Methods.* 2005;64(3):207-215.

21. Townsend W, Pasikowska M, Yallop D, et al. The architecture of neoplastic follicles in follicular lymphoma; analysis of the relationship between the tumor and follicular helper T-cells. *Haematologica.* 2019;105(6):1593-1603.

22. Amé-Thomas P, Tarte K. The yin and the yang of follicular lymphoma cell niches: role of microenvironment heterogeneity and plasticity. *Semin Cancer Biol.* 2014;24:23-32.

23. Haebe S, Shree T, Sathe A, et al. Single-cell analysis can define distinct evolution of tumor sites in follicularlymphoma. *Blood.* 2021;137(21):2869–2880.

24. Mir F, Barrington SF, Brown H, et al. Baseline SUVmax did not predict histological transformation in follicular lymphoma in the phase 3 GALLIUM study. *Blood.* 2020;135(15):1214-1218.

25. Koster A, Tromp HA, Raemaekers JM, et al. The prognostic significance of the intra-follicular tumor cell proliferative rate in follicular lymphoma. *Haematologica.* 2007;92(2):184-190.